

# Exact kinetic propagators for coherent state complex Langevin simulations

Thomas G. Kiely,<sup>1,\*</sup> Ethan C. McGarrigle,<sup>2,\*</sup> and Glenn H. Fredrickson<sup>2,3,4,†</sup>

<sup>1</sup>*Kavli Institute of Theoretical Physics, University of California, Santa Barbara, 93106, California, USA*

<sup>2</sup>*Department of Chemical Engineering, University of California, Santa Barbara, 93106, California, USA*

<sup>3</sup>*Materials Research Laboratory, University of California, Santa Barbara, 93106, California, USA*

<sup>4</sup>*Materials Department, University of California, Santa Barbara, 93106, California, USA*

(Dated: February 18, 2026)

We introduce and benchmark an improved algorithm for complex Langevin simulations of bosonic-coherent state path integrals. Our approach utilizes a Strang splitting of the imaginary-time propagator rather than the conventional linear-order Taylor expansion, allowing us to construct an action that incorporates higher-order terms at negligible computational cost. The resulting algorithm enjoys guaranteed linear stability independent of the imaginary-time discretization, enabling more resource-efficient simulations. We demonstrate this improved performance for single-species bosons and for two-component bosons with Rashba spin-orbit coupling.

## I. INTRODUCTION

Numerical path integral methods provide an exact approach for solving equilibrium quantum many-body problems, capturing the nontrivial interplay between quantum and thermal fluctuations [1–4]. These methods have had remarkable success at modeling interacting ensembles of bosons, with notable examples being superfluid  $^4\text{He}$  [5–9] and ultracold atom Bose-Einstein condensates (BECs) coupled to artificial gauge fields [10–13]. Path integral methods rely on a well-known mapping between a  $d$ -dimensional quantum partition function,  $\mathcal{Z} = \text{Tr}[\exp(-\beta \hat{H})]$ , and a  $(d+1)$ -dimensional classical path integral [14]. While the mapping is unambiguous in the continuum limit, numerical methods require one to discretize the path integral in the imaginary-time coordinate  $\tau \in (0, \beta)$ . There are many choices of how one constructs the discretized path integral; while all are equivalent in the continuum limit, this choice can drastically change the accuracy and stability of numerical methods. “Higher-order” discretized path integrals have been shown in various cases to improve numerical simulations [15], but these approaches require additional numerical resources. In this work we provide a general means of constructing numerically-stable coherent-state path integrals from bosonic quantum Hamiltonians without demanding any additional resources. Our method is complementary to higher-order constructions: It can seamlessly be integrated into these approaches, but it provides improved stability during complex Langevin sampling even at linear order. We benchmark our method in two experimentally-relevant scenarios: the single-component Bose gas and the two-component Bose gas with Rashba spin-orbit coupling.

Neutral atom arrays and Bose-Einstein condensates form a rich starting point for realizing various exotic states of matter, such as topological phases [16–19], su-

persolids [20–22], and quantum hall analog states [23]. These states are often theoretically understood in terms of simplified limits and toy models, such as the Laughlin state and the Toric code. Experimental realizations, however, rarely look so simple. Mean-field methods [24], which have had great success at modeling weakly-interacting BECs, introduce uncontrolled approximations when applied to these interacting and strongly-correlated systems.

Numerical path integral approaches, which treat quantum and thermal fluctuations on the same footing, provide a path towards numerically-exact and experimentally-realistic modeling of bosonic ensembles. One such technique, path integral Monte Carlo (PIMC) [25], uses Monte Carlo sampling over the coordinate basis to compute averages over the full path integral, requiring explicit exchange permutation sampling to enforce Bose statistics. This method provided some of the earliest successes in numerical path integral techniques [5–7] and has been used to study a wide range of strongly-interacting models in the continuum [8, 9] and lattice [26, 27] settings. The PIMC method, however, suffers from the sign problem and has generally been constrained to small system sizes of  $\lesssim 10^3$  particles.

Coherent state (CS) field theories with complex Langevin (CL) sampling [13, 28, 29] have emerged as a robust way to interrogate large bosonic assemblies with moderate interactions, regardless of whether a sign problem is present. Ultracold boson systems with artificial gauge fields [30] often introduce an explicit sign problem and constitute a natural application for CSCL. Heretofore, CSCL has enabled finite-temperature investigations of rotating BECs [10] and spin-orbit coupled BECs [11, 12]. In the case of isotropic two-dimensional “Rashba” spin-orbit coupling [30–32], the massive single-particle degeneracy greatly enhances the role of fluctuations, and CSCL has unveiled rich finite temperature behavior with a prediction of a quantum microemulsion analog [11, 33]. However, the applicability of CSCL is constrained by the memory cost of storing the coherent state fields in the resolved  $(d+1)$  space-imaginary time dimensions, where the standard first-order accurate the-

\* Equal contribution

† ghf@ucsb.edu

ory requires fine imaginary time discretizations to ensure convergent contributions to and unbiased sampling of the partition function [28].

In this work, we introduce a superior algorithm for performing CSCL simulations of continuum Bose fluids. Our method consists of a judicious second-order splitting of the imaginary-time propagator and utilizes the property that exponentials of quadratic operators,  $\exp(\hat{O})$ , map coherent states to coherent states. The resulting classical action incorporates many higher-order terms at a negligible computational cost and enjoys guaranteed linear numerical stability, independent of the imaginary-time discretization. We demonstrate the power and flexibility of this approach by applying it to a one-component Bose gas and to a two-component, two-dimensional Bose gas with Rashba spin-orbit coupling.

## II. PRELIMINARIES

Here, we utilize the complex Langevin method for simulating equilibrium coherent-state path integrals. Coherent state wavefunctions [34], which take the form  $|\phi\rangle = \exp\left(\sum_{\alpha} \phi(\alpha)\hat{\psi}^{\dagger}(\alpha)\right)|0\rangle$  where  $\hat{\psi}^{\dagger}(\alpha)$  is the boson creation operator in state  $\alpha$  [35] and  $\phi(\alpha)$  is a complex scalar field, constitute an overcomplete basis and admit a resolution of the identity. The equilibrium CS path integral is constructed by inserting  $N_{\tau}$  such identity operators into the partition function,  $\mathcal{Z} = \text{Tr}[e^{-\beta\hat{H}}]$ , where  $\hat{H}$  is a bosonic Hamiltonian and  $\beta = 1/k_B T$ . The partition function may then be rewritten as a path integral over the complex-conjugate fields  $\phi_j$  and  $\phi_j^*$ ,

$$\begin{aligned} \mathcal{Z} = \int \mathcal{D}(\phi^*, \phi) e^{-\sum_{j=0}^{N_{\tau}-1} \sum_{\alpha} \phi_j^*(\alpha)\phi_j(\alpha)} \\ \times \prod_{j=0}^{N_{\tau}-1} \langle \phi_j | e^{-\Delta\hat{H}} | \phi_{j-1} \rangle, \end{aligned} \quad (1)$$

weighted by matrix elements of the imaginary-time propagator. In the above we have defined an imaginary timestep  $\Delta = \beta/N_{\tau}$ , the periodic index  $j$  for distinct resolutions of the identity (i.e.  $\phi_{N_{\tau}} \equiv \phi_0$ ).

Numerical [13] and analytic [34, 36] approaches to studying the equilibrium path integral require a means of optimizing or sampling the field variables  $\phi_j(\alpha)$ . A systematic approach for doing this is to rewrite the partition function as  $\mathcal{Z} = \int \mathcal{D}(\phi^*, \phi) e^{-S[\phi^*, \phi]}$  in terms of an action functional  $S[\phi^*, \phi]$ . Given  $S[\phi^*, \phi]$ , both mean-field solutions and exact equilibrium thermodynamics can be accessed by the following descent scheme [28, 37]:

$$\frac{\partial \phi_j(\alpha)}{\partial t} = -\frac{\delta S[\phi, \phi^*]}{\delta \phi_j^*(\alpha)} + \eta_j(\alpha), \quad (2)$$

$$\frac{\partial \phi_j^*(\alpha)}{\partial t} = -\frac{\delta S[\phi, \phi^*]}{\delta \phi_j(\alpha)} + \eta_j^*(\alpha), \quad (3)$$

where  $\eta$  and  $\eta^*$  denote complex-conjugate noise sources with zero mean and unit variance [13]. Omitting the noise constitutes an imaginary-time relaxation algorithm to find  $\tau$  (or  $j$ )-independent saddle point solutions. Including the noise corresponds to a stochastic complex Langevin dynamics that provides unbiased sampling of the coherent state theory. State of the art algorithms for integrating Eqs. (2) and (3) invoke exponential time differencing (ETD) schemes that can be used to sample the stationary distribution  $\propto e^{-S}$  with accuracy up to  $\mathcal{O}(\Delta t^2)$ , where  $\Delta t$  is the Langevin timestep.

Constructing  $S[\phi^*, \phi]$  from Eq. (1) requires one to evaluate the matrix elements  $\langle \phi_j | e^{-\Delta\hat{H}} | \phi_{j-1} \rangle$ , which in most cases can only be done approximately. The textbook approach [13, 34] is to Taylor expand to linear order in  $\Delta$ . The expectation value  $\langle \phi_j | \hat{H} | \phi_{j-1} \rangle = \langle \phi_j | \phi_{j-1} \rangle H[\phi_j^*, \phi_{j-1}]$  is trivial after normal-ordering the bosonic field operators. Resumming the result, one finds

$$\langle \phi_j | e^{-\Delta\hat{H}} | \phi_{j-1} \rangle = \langle \phi_j | \phi_{j-1} \rangle e^{-\Delta H[\phi_j^*, \phi_{j-1}]} + \mathcal{O}(\Delta^2). \quad (4)$$

The action functional is then

$$\begin{aligned} S[\phi^*, \phi] = \sum_{j=0}^{N_{\tau}-1} \sum_{\alpha} \phi_j^*(\alpha)(\phi_j(\alpha) - \phi_{j-1}(\alpha)) \\ + \Delta \sum_{j=0}^{N_{\tau}-1} H[\phi_j^*, \phi_{j-1}] + \mathcal{O}(\Delta). \end{aligned} \quad (5)$$

where the overlap between coherent states has been inserted in the form  $\langle \phi_j | \phi_{j-1} \rangle = \exp[\sum_{\alpha} \phi_j^*(\alpha)\phi_{j-1}(\alpha)]$ . We note that the familiar (real-space) form of Eq. (5) is obtained by replacing  $\alpha \rightarrow \mathbf{r}$  and  $\sum_{\alpha} \rightarrow \int_V d^d r$ .

## III. IMPROVED ALGORITHM

The innovation in this work is the use of a more sophisticated approximation for evaluating the imaginary-time propagator. The resulting algorithm is still strictly linear-order in  $\Delta$ , but incorporates higher-order terms and exhibits favorable numerical stability properties for Langevin sampling. Our strategy starts from a second-order Strang splitting of the imaginary-time propagator,  $e^{-\Delta\hat{H}} = e^{-\Delta\hat{H}_0/2}e^{-\Delta\hat{H}_1}e^{-\Delta\hat{H}_0/2} + \mathcal{O}(\Delta^3)$ , where we have separated the Hamiltonian into two terms  $\hat{H} = \hat{H}_0 + \hat{H}_1$ . While this decomposition is generic, in the present case we require that (1)  $\hat{H}_0$  is quadratic in the bosonic creation/annihilation operators and (2) the minimum eigenvalue of  $\hat{H}_0$  is zero. Provided the spectrum is lower-bounded, the latter condition can always be fixed by adding and subtracting quadratic terms from  $\hat{H}_0$  and  $\hat{H}_1$ , respectively. Henceforth we will suggestively refer to  $\hat{H}_0$  as the *kinetic* term in the Hamiltonian and  $\hat{H}_1$  as the *interaction* term.

Provided that  $\hat{H}_0$  satisfies condition (1), we may *exactly* rewrite  $\langle \phi_j | e^{-\Delta\hat{H}_0/2}e^{-\Delta\hat{H}_1}e^{-\Delta\hat{H}_0/2} | \phi_{j-1} \rangle$  as

the expectation value of the interacting propagator,  $\langle \phi'_j | e^{-\Delta \hat{H}_1} | \phi'_{j-1} \rangle$ , with respect to transformed wavefunctions  $|\phi'_{j-1}\rangle = e^{-\Delta \hat{H}_0/2} |\phi_{j-1}\rangle$ . Importantly, the states  $|\phi'_j\rangle$  are still coherent states. Thus this approach requires minimal alterations to existing CSCL implementations.

It is most straightforward to construct the transformed wavefunctions in the eigenbasis of  $\hat{H}_0$ . In second-quantized notation, we define  $\hat{H}_0 = \sum_{\lambda} \epsilon_{\lambda} \hat{\psi}^{\dagger}(\lambda) \hat{\psi}(\lambda)$ . One may freely rewrite the coherent state wavefunction in this basis,  $\exp(\sum_{\lambda} \phi(\lambda) \hat{\psi}^{\dagger}(\lambda)) |0\rangle$ , using the unitary matrix  $U_{\alpha, \lambda}^{\dagger} = \langle 0 | \hat{\psi}(\alpha) \hat{\psi}^{\dagger}(\lambda) | 0 \rangle$  [38]. The transformed wavefunction is then given by [38–40]

$$|\phi'\rangle = \exp \left( \sum_{\lambda} e^{-\Delta \epsilon_{\lambda}/2} \phi(\lambda) \hat{\psi}^{\dagger}(\lambda) \right) |0\rangle \quad (6)$$

$$\langle \phi' | = \langle 0 | \exp \left( \sum_{\lambda} e^{-\Delta \epsilon_{\lambda}/2} \phi^*(\lambda) \hat{\psi}(\lambda) \right) \quad (7)$$

Henceforth we will refer to the transformed fields themselves, which are defined in the diagonal basis as  $\phi'(\lambda) = e^{-\Delta \epsilon_{\lambda}/2} \phi(\lambda)$  but may be subsequently transformed into other bases throughout the calculation.

We evaluate the resulting matrix element,  $\langle \phi'_j | e^{-\Delta \hat{H}_1} | \phi'_{j-1} \rangle$ , using the conventional linear-order Taylor expansion, but now with respect to the transformed CS wavefunctions:

$$\langle \phi'_j | e^{-\Delta \hat{H}_1} | \phi'_{j-1} \rangle = \langle \phi'_j | \phi'_{j-1} \rangle e^{-\Delta H_1[(\phi_j^*, \phi_{j-1})']} + \mathcal{O}(\Delta^2) \quad (8)$$

The resulting action functional,

$$S[\phi^*, \phi] = \sum_{j=0}^{N_{\tau}-1} \sum_{\lambda} \phi_j^*(\lambda) [\phi_j(\lambda) - e^{-\Delta \epsilon_{\lambda}} \phi_{j-1}(\lambda)] + \Delta \sum_{j=0}^{N_{\tau}-1} H_1[(\phi_j^*, \phi_{j-1})'], \quad (9)$$

is accurate to linear order in  $\Delta$ , like Eq. (5), but incorporates many higher-order terms without introducing significant algorithmic costs. For example, Eq. (9) is exact to all orders in  $\Delta$  if  $\hat{H}_1 = 0$ , with an example calculation shown in [38] where observables are independent of  $\Delta$ . We emphasize that  $H_1$  is a functional of the *transformed* fields, so functional derivatives of this term in the action (as appear in Eqs. (2) and (3)) will include a Jacobian factor, with an example detailed in [38].

This exact treatment of the kinetic term has important implications for the stability of the Langevin dynamics. The quadratic term in the action contributes a term  $\sum_l A_{jl} \phi_l$  to the equation of motion for  $\phi_j$  (see Eq. (2) and similar for  $\phi_j \leftrightarrow \phi_j^*$ ). Linear stability of the algorithm is determined by the signs of the eigenvalues of  $A$ . For the improved action functional in Eq. (9), the algorithm is linearly stable if  $\text{Re}[1 \pm e^{-\Delta \epsilon_{\lambda}}] \geq 0 \forall \lambda$ . Thus the algorithm enjoys absolute linear stability if  $\hat{H}_0$

has a positive (semi-)definite spectrum (see condition (2) above). By contrast, the action functional in Eq. (5) requires  $\text{Re}[1 \pm (1 - \Delta \epsilon_{\lambda})] \geq 0 \forall \lambda$ , and hence is only stable for sufficiently small  $\Delta = \beta/N_{\tau}$ . Stability in the original approach then requires more  $N_{\tau}$  discretization, making the method more resource-intensive as the required memory to store the CS fields and computation time per CL step increases. This stability constraint is exacerbated when using a fine spatial grid to model translationally-invariant systems, as this requires the incorporation of large-momentum (high-energy) modes.

In order to compute observables,  $\langle \hat{O}(\mathbf{r}) \rangle$ , one introduces an additional term to the Hamiltonian,  $\hat{H}_J = -\beta^{-1} \int d\mathbf{r} J(\mathbf{r}) \hat{O}(\mathbf{r})$ . This endows the partition function  $\mathcal{Z}[J]$  with a dependence on the source fields,  $J(\mathbf{r})$ . The expectation value is obtained as  $\langle \hat{O}(\mathbf{r}) \rangle = \delta \ln \mathcal{Z}[J]/\delta J(\mathbf{r})|_{J(\mathbf{r}) \rightarrow 0}$ . In practical CSCL simulation, this procedure yields an analytic expression for a functional  $O[\phi, \phi^*]$  whose average with respect to the CS path integral is  $\langle \hat{O}(\mathbf{r}) \rangle$  [13]. As we show in Ref. [38], the functionals for computing observable expectation values in this manner retain the same form as in the primitive method, but with respect to the transformed fields rather than the bare fields:  $\tilde{O}[\phi, \phi^*] = O[(\phi, \phi^*)']$ .

#### IV. RESULTS

To benchmark the performance of Eq. (9), we first consider a two-dimensional (2D) interacting Bose gas. The Hamiltonian may be written as  $\hat{H}_0 + \hat{H}_1$  with

$$\hat{H}_0 = \int d\mathbf{r} \hat{\psi}^{\dagger}(\mathbf{r}) \left( -\frac{\hbar^2}{2m} \nabla^2 \right) \hat{\psi}(\mathbf{r}) \quad (10)$$

$$\hat{H}_1 = \frac{1}{2} \int d\mathbf{r} \int d\mathbf{r}' \hat{\psi}^{\dagger}(\mathbf{r}) \hat{\psi}^{\dagger}(\mathbf{r}') u(\mathbf{r} - \mathbf{r}') \hat{\psi}(\mathbf{r}) \hat{\psi}(\mathbf{r}'), \quad (11)$$

where in our grand canonical formulation, we include the chemical potential contribution in  $\hat{H}_1 \rightarrow \hat{H}_1 - \mu \hat{N}$ . Here  $\hat{H}_0$  is diagonalized with a Fourier transform, so our diagonal basis is  $\lambda \equiv \mathbf{k}$  with eigenvalues  $\epsilon(\mathbf{k}) = \hbar^2 k^2 / 2m$ . Throughout this work we consider a delta function pseudopotential  $u(\mathbf{r} - \mathbf{r}') = g \delta(\mathbf{r} - \mathbf{r}')$ , a good approximation for s-wave collisions between ultracold atoms, where the strength  $g$  is directly related to the s-wave scattering length  $a_s$  via  $g_{3D} = 4\pi \hbar^2 a_s / m$  [24]. We emphasize that our technique applies equally well to long-range interactions. We present the results in dimensionless form, rescaled by the healing length  $\ell = (\hbar^2 / 2m\mu)^{1/2}$  and chemical potential  $\mu$  such that  $\bar{\beta} = \beta\mu$  constitutes a dimensionless inverse temperature. For both examples below, we use two-dimensional simulations that assume a quasi-2D environment with axial length scale  $\ell_z = \sqrt{\hbar/m\omega_z}$  with  $\omega_z$  an axial harmonic trapping frequency. As such, an effective two-dimensional repulsive coupling constant is determined by  $g_{2D} = g_{3D} / \sqrt{2\pi\ell_z}$ , leading to a dimensionless constant  $\bar{g}_{2D} = 2mg_{2D}/\hbar^2$ .

We perform simulations in periodic cells with rescaled sizes  $\bar{L}_\nu = L_\nu/\ell$  in each direction  $\nu = x, y$ .

In Fig. (1) we show the results of a CSCL simulation of the 2D Bose gas using our new approach (in gold) as well as the “primitive” first-order approach (Eq. (5); in maroon) for various  $N_\tau$  and  $\bar{\beta} = 0.5$ ,  $\bar{g}_{2D} = 0.0165$ . We find that the primitive approach requires  $N_\tau > 72$  to achieve numerical stability. Our new approach, by contrast, is numerically stable down to the smallest  $N_\tau$  sampled here ( $N_\tau = 4$ ). The two methods show excellent agreement at large  $N_\tau$ , with the new approach maintaining accuracy within 0.2 % for the particle number out to very coarse imaginary time resolutions (small  $N_\tau$ ). The small numerical difference in canonical internal energy  $U - \mu N$  and the grand free energy  $\Omega$  in Fig. (1) highlights the low entropy per particle in the superfluid phase with quasi-long range order.

We now consider a nontrivial example with an explicit sign problem: a two-component, two-dimensional Bose fluid with Rashba spin-orbit coupling. The Hamiltonian is

$$\hat{H}_0 = \frac{1}{2m} \sum_{\alpha\gamma} \int d\mathbf{r} \hat{\psi}_\alpha^\dagger(\mathbf{r}) (\delta_{\alpha\gamma} i\hbar\nabla - \mathcal{A}_{\alpha\gamma})^2 \hat{\psi}_\gamma(\mathbf{r}) \quad (12)$$

$$\hat{H}_1 = \sum_{\alpha\gamma} \frac{g_{\alpha\gamma}}{2} \int d\mathbf{r} \hat{\psi}_\alpha^\dagger(\mathbf{r}) \hat{\psi}_\gamma^\dagger(\mathbf{r}) \hat{\psi}_\gamma(\mathbf{r}) \hat{\psi}_\alpha(\mathbf{r}) \quad (13)$$

where  $\alpha, \gamma$  are spin indices and  $g_{\alpha\gamma} = g_{2D}(\delta_{\alpha\gamma} + \eta(1 - \delta_{\alpha\gamma}))$  is a symmetric spin-dependent contact interaction strength, where  $\eta > 1$  ( $< 1$ ) denotes immiscible (miscible) conditions between the two components. The vector potential is given by  $\mathcal{A}_{\alpha\gamma} = \hbar\kappa(\sigma_{\alpha\gamma}^x \hat{x} + \sigma_{\alpha\gamma}^y \hat{y})$  where  $\sigma_{\alpha\gamma}^a$  are matrix elements of the Pauli vectors in spin space ( $a = x, y, z$ ). The kinetic term  $\hat{H}_0$  has two bands with eigenvalues  $\epsilon_\pm(\mathbf{k}) = \hbar^2(k^2 \pm 2\kappa|\mathbf{k}|)/2m$ . Following Ref. [11], we report our results in a dimensionless form defined by the characteristic energy  $\mu_{\text{eff}} = \mu - \hbar^2\kappa^2/m$  and healing length  $\ell = (\hbar^2/2m\mu_{\text{eff}})^{-1/2}$ . This procedure yields a dimensionless SOC strength  $\bar{\kappa} = \kappa\ell$ . See Ref. [38] for more details on our implementation.

Our new approach requires us to work in the eigenbasis of  $\hat{H}_0$  (see Ref. [38] for details for building the coherent state path integral and corresponding CL algorithm). We furthermore must shift  $\hat{H}_0$  such that it is positive-definite; this is achieved by an unbiased shift  $\hat{H}_0 \rightarrow \hat{H}_0 + \mu' \hat{N}$ ,  $\hat{H}_1 \rightarrow \hat{H}_1 - \mu' \hat{N}$  so that  $\hat{H} = \hat{H}_0 + \hat{H}_1$  remains unchanged. As such, we set  $\mu' = \min_{\mathbf{k}} \epsilon_-(\mathbf{k}) = \bar{\kappa}^2$ .

In Fig. (2) we show the results of CSCL simulations of the 2D Rashba spin-orbit-coupled Bose gas, contrasting our new approach (in gold) with the primitive propagator (in maroon) for various  $N_\tau$ . Here the system is in a superfluid stripe phase with smectic spin order [11]. We find that the primitive approach becomes unstable for  $N_\tau \leq 35$ , while again the new approach remains stable down to remarkably coarse imaginary-time grids ( $N_\tau = 4$ ). We observe good convergence for the new method as  $N_\tau$  increases, noting that the observable esti-

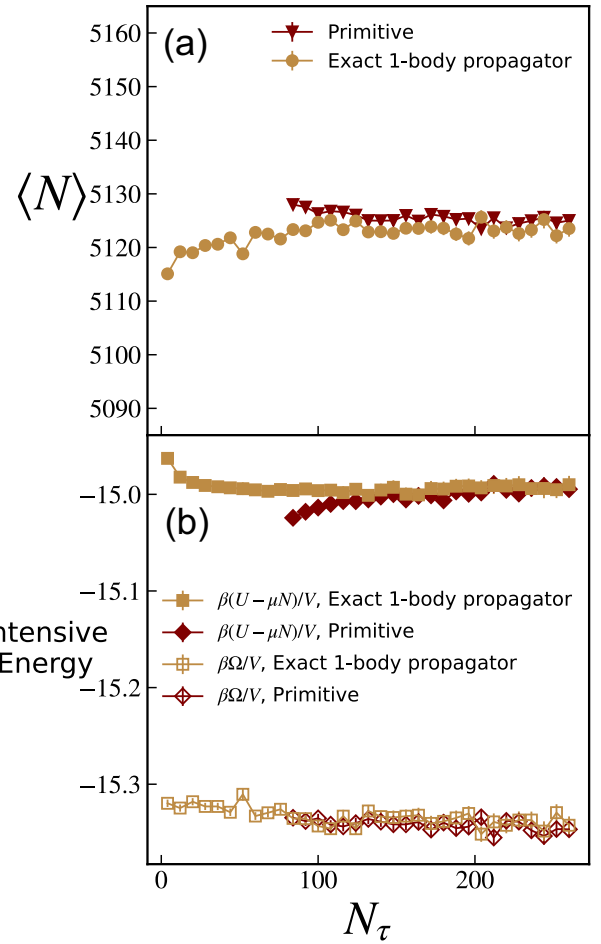


FIG. 1. Demonstration of  $N_\tau$  convergence on a single component, two-dimensional Bose gas with contact interactions  $\bar{g}_{2D} = 0.0165$  at  $\bar{T} = \bar{\beta}^{-1} = 2.0$ . Convergence plots for the a) particle number as well as the b) intensive canonical internal energy (filled markers) and grand free energy (open markers), showing the standard first order “primitive” treatment with maroon diamonds and the exact one-body propagator method introduced in this work with gold squares. At lower  $N_\tau$ , the missing primitive data is due to numerical instabilities where data cannot be collected. Simulations used the ETD algorithm with  $\Delta t = 0.005$  and were conducted in a square cell with side length  $\bar{L} = 9.19$  with  $N_x = 36$  plane waves in each direction.

mates at small  $N_\tau$  show less than 1% deviation from the large  $N_\tau$  value. In Figure (2b), the primitive estimate of the internal energy converges more slowly than our new approach.

## V. DISCUSSION

The demonstrations in Figures (1) and (2) represent a significant improvement in method efficiency. With the simple change proposed here, the same thermodynamic results are obtained with significantly reduced computational cost. The reduction in required  $N_\tau$  leads to appre-

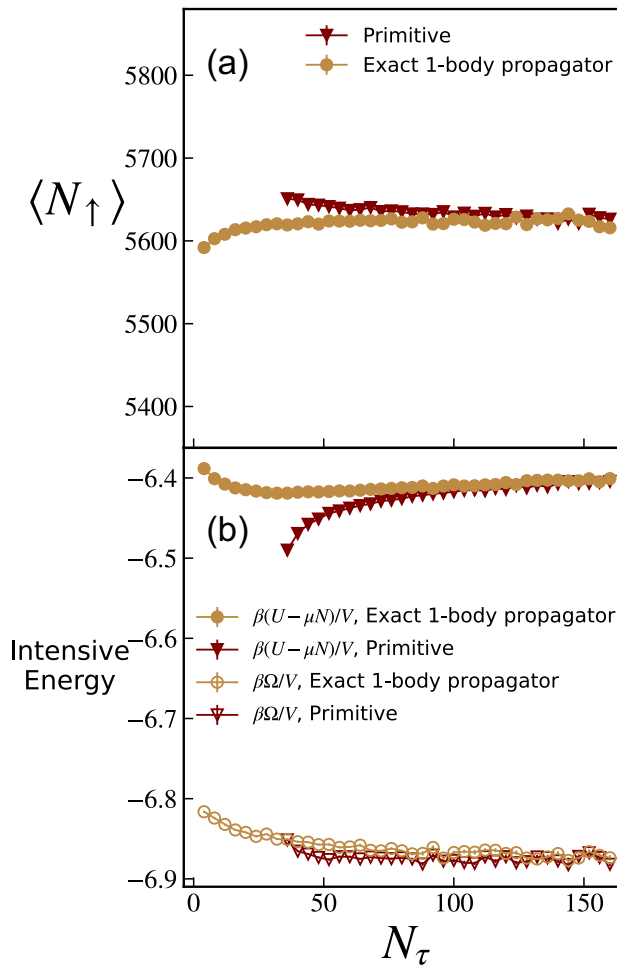


FIG. 2. Demonstration of  $N_\tau$  convergence on a two-component, two-dimensional Rashba spin-orbit coupled Bose gas in the stripe phase with contact interactions  $\bar{g}_{2D} = 0.1$  at  $\bar{T} = \bar{\beta}^{-1} = 1.0$  in immiscible conditions ( $\eta = 1.1$ ). Convergence plots for the a) particle number as well as the b) intensive canonical internal energy (filled markers) and grand free energy (open markers), showing the standard first order “primitive” treatment with maroon triangles and the exact one-body propagator method with gold circles. At lower  $N_\tau$ , we note missing primitive data due to numerical instabilities where data cannot be collected. Simulations used the ETD algorithm with  $\Delta t = 0.01$  and were conducted in a square cell with side length  $\bar{L} = 10\pi$  with  $N_x = 56$  plane waves in each direction.

ciable savings in both memory and in computation time per CL step. In bypassing the linear stability requirement from the primitive method, the new propagator treatment permits high-resolution simulations of bosonic matter down to very low temperatures.

The case of Rashba SOC presents an example where diagonalizing during the path integral procedure leads to efficiency improvements when conducting Langevin sampling downstream. Since the Langevin SOC drift terms are diagonal in the dressed state basis, ETD algorithms are efficient and integrate the SOC terms to all orders

in  $\Delta t$ . The improved accuracy and stability of this approach could enable efficient simulations of strongly spin-orbit coupled bosons ( $\kappa \gg 1$ ), where rich phenomena are speculated [41, 42].

As noted earlier, resolution in the imaginary time direction is not only important for low-temperature calculations. The stability requirement for a standard Trotterization of the kinetic term can also be saturated at fixed temperature by increasing the spatial resolution and hence the sampling of high-momentum modes. A similar feature emerges when simulating Bose fluids in an optical trap, which is necessary for precise correspondence with ultracold atom experiments. The guaranteed linear stability of the present algorithm is therefore of significant practical value in virtually every CSCL simulation.

## VI. CONCLUSION

We conclude by emphasizing that the approach outlined here is complementary to many other techniques for taming numerical path integrals. Our approach can be used in higher-order decompositions [15, 43] of  $e^{-\Delta \hat{H}}$  wherever one seeks to apply a quadratic operator to a coherent state. Furthermore, our treatment of quadratic propagators may enable a more robust incorporation of quadratic constraints, such as fixed particle number in the canonical ensemble [44], by performing the projections within the path integral.

Boson models with strong interactions still present a formidable challenge for CSCL approaches with our improved propagator method. Strong pairwise interactions produce frequent nonlinear numerical instabilities that result in method failure. However, a potential path forward would first decouple the quartic interaction via auxiliary fields from a Hubbard-Stratonovich transformation, and then proceed with Strang splitting and our quadratic propagator procedure. The resulting hybrid coherent state - auxiliary field theory would be second-order accurate and may exhibit superior numerical stability when sampling strongly interacting boson models. Finally we note that this approach is not limited to decompositions of imaginary-time propagators, and indeed can be readily applied to real-time contours in order to simulate quantum many-body dynamics (via Keldysh contours) [13, 45] or classical many-body dynamics in the Doi-Peliti coherent states representation [46–48].

## ACKNOWLEDGEMENTS

This work was enabled by field-theoretic simulation tools developed under support from the National Science Foundation (CMMT Program, DMR-2104255). Use was made of computational facilities purchased with funds from the NSF (CNS-1725797) and administered by the Center for Scientific Computing (CSC). This work made use of the BioPACIFIC Materials Innovation Platform

computing resources of the National Science Foundation Award No. DMR-1933487. The CSC is supported by the California NanoSystems Institute and the Materials Research Science and Engineering Center (MRSEC; NSF DMR 2308708) at UC Santa Barbara. E.C.M acknowledges support from a Mitsubishi Chemical Fellowship. TGK acknowledges support from the National Science Foundation under grant PHY-2309135 to the Kavli Institute for Theoretical Physics (KITP), and from the Gordon and Betty Moore Foundation through Grant GBMF8690 to the University of California, Santa Barbara.

### Appendix A: Quadratic propagation of coherent state wavefunction

Here we show that  $e^{-\Delta\hat{H}_0/2}|\phi\rangle$ , where  $\hat{H}_0$  is a quadratic (bosonic) Hamiltonian and  $|\phi\rangle$  is a coherent state, may be expressed as another coherent state,  $|\phi'\rangle$ , with transformed complex field variables. We start by defining the single-particle eigenbasis of  $\hat{H}_0$ :  $\hat{H}_0|\lambda\rangle = \epsilon_\lambda|\lambda\rangle$  with  $|\lambda\rangle \equiv \hat{a}_\lambda^\dagger|0\rangle$ . This defines a unitary matrix  $U_{\alpha,\lambda}^\dagger = \langle\alpha|\lambda\rangle$  that diagonalizes the single-particle Hamiltonian. We then rewrite  $|\phi\rangle$  in the eigenbasis of  $\hat{H}_0$ :  $\exp(\sum_\lambda \phi(\lambda)\hat{a}_\lambda^\dagger)|0\rangle$ . Note that this change of basis does not alter the form of the coherent-state wavefunction:

$$\sum_\alpha \phi(\alpha)\hat{a}_\alpha^\dagger = \sum_{\alpha,\lambda_1,\lambda_2} \phi(\lambda_1)U_{\lambda_1,\alpha}U_{\alpha,\lambda_2}^\dagger\hat{a}_{\lambda_2}^\dagger \quad (\text{A1})$$

$$= \sum_{\lambda_1,\lambda_2} \phi(\lambda_1)\delta_{\lambda_1,\lambda_2}\hat{a}_{\lambda_2}^\dagger \quad (\text{A2})$$

$$= \sum_\lambda \phi(\lambda)\hat{a}_\lambda^\dagger \quad (\text{A3})$$

The transformed state is defined as

$$|\phi'\rangle = e^{-\Delta\hat{H}_0/2} \exp\left(\sum_\lambda \phi(\lambda)\hat{a}_\lambda^\dagger\right)|0\rangle \quad (\text{A4})$$

We now use the condition of a trivial vacuum state,  $e^{-\Delta\hat{H}_0/2}|0\rangle = |0\rangle$ , to insert an inverse kinetic propagator in front of the vacuum state:

$$|\phi'\rangle = e^{-\Delta\hat{H}_0/2} \exp\left(\sum_\lambda \phi(\lambda)\hat{a}_\lambda^\dagger\right) e^{\Delta\hat{H}_0/2}|0\rangle. \quad (\text{A5})$$

We may pull the factors of  $e^{\pm\Delta\hat{H}_0/2}$  into the exponential:

$$|\phi'\rangle = \exp\left(e^{-\Delta\hat{H}_0/2} \sum_\lambda \phi(\lambda)\hat{a}_\lambda^\dagger e^{\Delta\hat{H}_0/2}\right)|0\rangle \quad (\text{A6})$$

Finally, using the second-quantized form  $\hat{H}_0 = \sum_\lambda \epsilon_\lambda n_\lambda$ , the propagators may be commuted through the sum to find:

$$|\phi'\rangle = \exp\left(\sum_\lambda e^{-\Delta\epsilon_\lambda/2}\phi(\lambda)\hat{a}_\lambda^\dagger\right)|0\rangle \quad (\text{A7})$$

Thus we have shown that  $|\phi'$  is a coherent state wavefunction that is related to  $|\phi\rangle$  by a transformation of the complex field variables in the eigenbasis of  $\hat{H}_0$ :  $\phi'(\lambda) = e^{-\Delta\epsilon_\lambda/2}\phi(\lambda)$ . Following these same steps, it is straightforward to derive that  $\langle\phi|e^{-\Delta\hat{H}_0/2} = \langle\phi'|$  is a coherent state defined by the transformation  $(\phi^*(\lambda))' = e^{-\Delta\epsilon_\lambda/2}\phi^*(\lambda)$ .

The case of non-interacting bosons provides a useful benchmark that highlights the efficacy of this approach. In the non-interacting limit ( $g = 0$ ), no Strang splitting error is incurred nor is Trotterization required, as the kinetic propagator  $e^{-\beta\hat{H}_0}$  can be applied exactly to all orders in  $\beta$  using the kinetic-propagated basis  $|\phi'\rangle$ . As a result, the ideal gas partition function is obtained after performing Gaussian integrals over the coherent state amplitudes *without invoking the usual  $N_\tau \rightarrow \infty$  limit* [34]. As a result, simulations of non-interacting bosons show no  $N_\tau$  dependence in their observables, underscoring the exactness of our approach.

Shown in Figure (3), the particle number and internal energy observables are independent of the imaginary time discretization and enjoy absolute numerical stability. We readily compare results for non-interacting bosons with known thermodynamic references, which are computed by an explicit summation over wavevector states:

$$\begin{aligned} \langle N \rangle &= \sum_{\mathbf{k}} \frac{1}{e^{\beta(\epsilon_{\mathbf{k}} - \mu)} - 1} \\ \langle U \rangle &= \sum_{\mathbf{k}} \frac{\epsilon_{\mathbf{k}}}{e^{\beta(\epsilon_{\mathbf{k}} - \mu)} - 1} \end{aligned} \quad (\text{A8})$$

where  $\epsilon_{\mathbf{k}} = \hbar^2\mathbf{k}^2/2m$  is the continuum kinetic dispersion and a suitably large momentum cutoff is chosen such that the sum converges. The thermodynamic results of equations (A8) are derived from the partition function and are valid in any spatial dimensionality. The agreement of both methods with the analytical reference serves to simultaneously validate our exact propagator method while highlighting its favorable numerical stability and accuracy properties.

### Appendix B: Extension to Pseudospin-1/2 Coherent States with Rashba Spin-orbit Coupling

Here we detail the applicability of our approach to multicomponent systems with a non-trivial one-body spectra. Using two-photon Raman transitions coupled with a biasing magnetic field, it is possible to create a system Pseudospin-1/2 bosons from a  $S = 1$  boson system [49]. Furthermore, with additional Raman lasers [19, 50], it is possible to imbue the system with a two-dimensional isotropic ‘‘Rashba’’ spin-orbit coupling. The Rashba coupling constitutes a fascinating case of great fundamental interest due to the massive single particle degeneracy of the Rashba Hamiltonian. Here, a degenerate ring of states appears with radius  $|\mathbf{k}| = \kappa$ , with  $\kappa$  taken as the

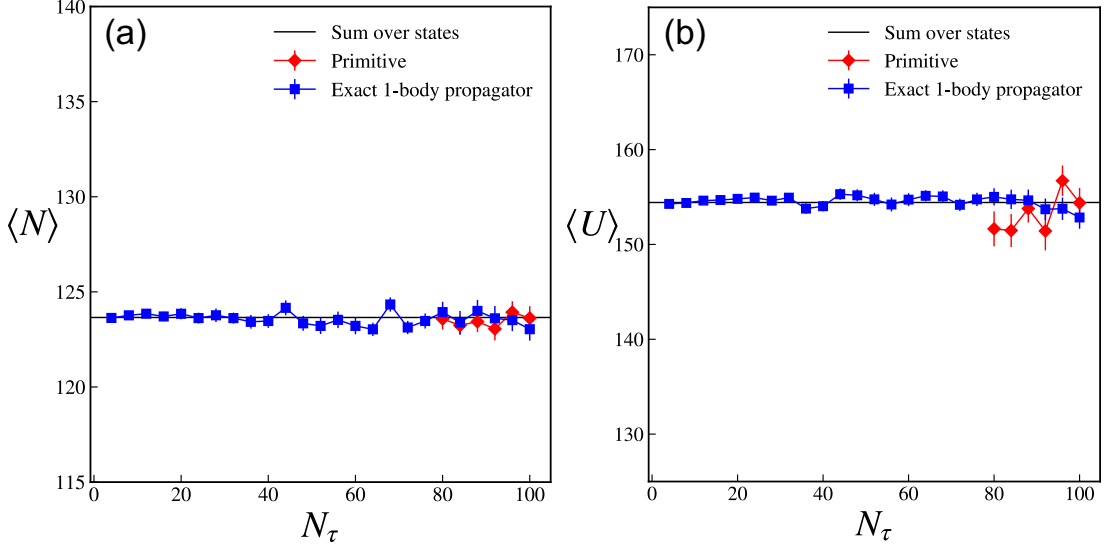


FIG. 3. Imaginary time dependence of ideal Bose gas simulations. Ensemble-averaged a) particle number and b) internal energy as a function of imaginary time discretization  $N_\tau$  for the primitive method (red diamonds) and the new exact propagator method (blue squares) introduced in this manuscript. The black solid line denotes the exact thermodynamic reference for the ideal Bose gas, computed using a sum over wavevector basis states with sufficient momentum cutoff. Data from the primitive data below  $N_\tau = 80$  are not shown due to numerical instability, which prevents meaningful data collection. Simulations consisted of a two-dimensional ensemble of non-interacting bosons with  $\bar{g}_{2D} = 0$ ,  $\ell = \sqrt{\hbar^2/2m|\mu|} = 4.29$ ,  $\mu = -0.33$  K,  $\beta = 0.50$  K $^{-1}$ ,  $L_x/\ell = L_y/\ell = 11.67$ , and  $N_x = N_y = 80$  grid points in each direction. The exponential-time-differencing (ETD) numerical algorithm was used with a Langevin step discretization  $\Delta t = 0.0033$ . Error bars depict standard errors of the mean, determined during sample averaging.

spin-orbit coupling strength. The SOC Hamiltonian can be expressed in a compact vectorized form:

$$\hat{H}_{\text{SOC}} = \int d^2r \hat{\Psi}^\dagger \left[ \frac{1}{2m} (\hat{p}_\perp^2 - \mathcal{A})^2 \right] \hat{\Psi} \quad (\text{B1})$$

where  $\hat{\Psi} = (\hat{\psi}_\uparrow(\mathbf{r}), \hat{\psi}_\downarrow(\mathbf{r}))^T$  is a two-component vector of second-quantized field operators satisfying Bose commutation relations [34].

After rescaling by the healing length as in reference [11] and incorporating the necessary chemical potential shift  $\mu'$  to ensure a positive definite spectrum, the resulting rank-2 Rashba Hamiltonian matrix can be written as  $\hat{H}_{\text{SOC}}/\mu_{\text{eff}} = \sum_{\mathbf{k}} \hat{\Psi}_{\mathbf{k}}^\dagger K_{\mathbf{k}} \hat{\Psi}_{\mathbf{k}}$ . The one-body matrix  $K_{\mathbf{k}}$  has diagonal elements  $K_{\alpha\alpha} = \mathbf{k}^2 + \mu'$  for both  $\alpha = \uparrow, \downarrow$  and off-diagonal elements  $K_{\uparrow\downarrow} = -2\kappa|\mathbf{k}|e^{-i\theta_{\mathbf{k}}}$  and  $K_{\downarrow\uparrow} = K_{\uparrow\downarrow}^*$ , with  $\theta_{\mathbf{k}} = \arctan(k_y/k_x)$ . This can be diagonalized by a unitary transformation  $U_{\mathbf{k}}$  to yield  $D_{\mathbf{k}} = U_{\mathbf{k}} K_{\mathbf{k}} U_{\mathbf{k}}^\dagger$ , where  $D_{\mathbf{k}}$  is a diagonal matrix with entries  $D_{00} = E_+(\mathbf{k})$  and  $D_{11} = E_-(\mathbf{k})$ . The unitary transformation involves eigenvectors  $U_{\mathbf{k}} = [v_{+,\mathbf{k}}, v_{-,\mathbf{k}}]$ , which are defined  $v_{+,\mathbf{k}} = 2^{-1/2}(1, -\exp(\theta_{\mathbf{k}}))^T$  and  $v_{-,\mathbf{k}} = 2^{-1/2}(1, \exp(\theta_{\mathbf{k}}))^T$ . The eigenvalue spectrum is  $E_{\pm}(\mathbf{k}) = \mathbf{k}^2 \pm 2\kappa|\mathbf{k}| + \mu'$ . Thus, the Hamiltonian is easily re-expressed as  $\hat{H}_{\text{SOC}}/\mu_{\text{eff}} = \sum_{\mathbf{k}} \tilde{\Psi}_{\mathbf{k}}^\dagger D_{\mathbf{k}} \tilde{\Psi}_{\mathbf{k}}$ , where we have switched to a diagonal ‘‘dressed state’’ field operator basis:  $\tilde{\Psi}_{\mathbf{k}} = U_{\mathbf{k}} \hat{\Psi}_{\mathbf{k}}$  and  $\tilde{\Psi}_{\mathbf{k}}^\dagger = \hat{\Psi}_{\mathbf{k}}^\dagger U_{\mathbf{k}}^\dagger$ . Instead of pseudospin states, the field operator components represent helicity states  $|\pm; \mathbf{k}\rangle$  that correspond with the bands  $E_{\pm}(\mathbf{k})$ .

When building the coherent state path integral for Rashba bosons, the unitary transformation  $U_{\mathbf{k}}$  yields dressed coherent state vectors  $\tilde{\phi}_{\mathbf{k}} = U_{\mathbf{k}} \phi_{\mathbf{k}}$  and  $\tilde{\phi}_{\mathbf{k}}^\dagger = \phi_{\mathbf{k}}^\dagger U_{\mathbf{k}}^\dagger$  with no change in the functional integration measure, identity resolution, or coherent state amplitudes:  $|\phi_j\rangle = \exp(\sum_{\mathbf{k}} \tilde{b}_{\mathbf{k}}^\dagger \phi_{\mathbf{k}}) |0\rangle = \exp(\sum_{\mathbf{k}} \tilde{b}_{\mathbf{k}}^\dagger U_{\mathbf{k}} U_{\mathbf{k}}^\dagger \phi_{\mathbf{k}}) |0\rangle = \exp(\sum_{\mathbf{k}} \tilde{b}_{\mathbf{k}}^\dagger \tilde{\phi}_{\mathbf{k}}) |0\rangle$ . We apply the Strang splitting for the propagator in each matrix element  $\langle \phi_j | e^{-\Delta \hat{H}} | \phi_{j-1} \rangle = \langle \phi_j | e^{-\Delta \hat{H}_{\text{SOC}}/2} e^{-\Delta \hat{H}_{\text{int}}} e^{-\Delta \hat{H}_{\text{SOC}}/2} | \phi_{j-1} \rangle + \mathcal{O}(\Delta_\tau^3)$  and then evaluate the SOC propagator on the the coherent state exactly:

$$\begin{aligned} e^{-\Delta \hat{H}_{\text{SOC}}/2} |\phi_j\rangle &= e^{-\Delta/2 \sum_{\mathbf{k}} \tilde{\Psi}_{\mathbf{k}}^\dagger D_{\mathbf{k}} \tilde{\Psi}_{\mathbf{k}}} |\phi_j\rangle \\ &= e^{-\Delta/2 \sum_{\mathbf{k}} \tilde{\Psi}_{\mathbf{k}}^\dagger D_{\mathbf{k}} \tilde{\Psi}_{\mathbf{k}}} e^{\sum_{\mathbf{k}} \tilde{b}_{\mathbf{k}}^\dagger \tilde{\phi}_{\mathbf{k}}} |0\rangle \\ &= \exp\left(\sum_{\mathbf{k}} \tilde{b}_{\mathbf{k}}^\dagger e^{-\Delta D_{\mathbf{k}}/2} \tilde{\phi}_{\mathbf{k}}\right) |0\rangle \\ &\equiv |\phi'_j\rangle \end{aligned}$$

where we have safely leveraged the previous insights since the dressed bosons obey the usual commutation relations  $[\hat{b}_{\alpha',\mathbf{k}}, \hat{b}_{\gamma',\mathbf{k}'}^\dagger] = \delta_{\mathbf{k},\mathbf{k}'} \delta_{\alpha',\gamma'}$ , with  $\alpha'$  denoting a dressed state index.

Therefore, we can proceed, but care must be taken with the interaction Hamiltonian, which is composed of density-density interactions written in the pseudospin basis.

$$\langle \phi_j | e^{-\Delta \hat{H}} | \phi_{j-1} \rangle = \langle \phi'_j | e^{-\Delta \hat{H}_{\text{int}}} | \phi'_{j-1} \rangle \quad (\text{B2})$$

In the usual first-order Taylor expansion, we encounter terms where operators in the pseudospin basis must be evaluated with dressed coherent states, such as  $\langle \phi'_j | \hat{b}_\gamma^\dagger \hat{b}_\alpha^\dagger \hat{b}_\gamma \hat{b}_\alpha | \phi'_{j-1} \rangle$ . We evaluate them as such:

$$\hat{b}_{\alpha,\mathbf{k}} |\phi'_j\rangle = \sum_{\gamma'} (U_{\mathbf{k}})_{\alpha\gamma'} \tilde{b}_{\gamma',\mathbf{k}} |\phi'_j\rangle \quad (\text{B3})$$

$$= \sum_{\gamma'} (U_{\mathbf{k}})_{\alpha\gamma'} \tilde{\phi}'_{\gamma',j,\mathbf{k}} |\phi'_j\rangle \quad (\text{B4})$$

$$= \phi'_{\alpha,j,\mathbf{k}} |\phi'_j\rangle \quad (\text{B5})$$

where we have defined a coherent state amplitude in the pseudospin basis that's been propagated forward with the kinetic energy operator.

Now, we show that the field operator in the pseudospin basis acting on  $|\phi'_j\rangle$  yields the following:

$$\hat{\psi}_\alpha(\mathbf{r}) |\phi'_j\rangle = \sum_{\mathbf{k}} \psi_\alpha(\mathbf{r}) b_{\alpha,\mathbf{k}} |\phi'_j\rangle \quad (\text{B6})$$

$$= \sum_{\mathbf{k}} \psi_\alpha(\mathbf{r}) \phi'_{\alpha,j,\mathbf{k}} |\phi'_j\rangle \quad (\text{B7})$$

$$= \phi'_{\alpha,j}(\mathbf{r}) |\phi'_j\rangle, \quad (\text{B8})$$

where in practice we would compute this propagated pseudospin coherent state via the following procedure:

$$\phi'_j(\mathbf{r}) = \mathcal{F}_{\mathbf{k} \rightarrow \mathbf{r}}^{-1} \left[ U_{\mathbf{k}}(e^{-\Delta D_{\mathbf{k}}/2} \tilde{\phi}) \right] \quad (\text{B9})$$

$$= \mathcal{F}_{\mathbf{k} \rightarrow \mathbf{r}}^{-1} \left[ U_{\mathbf{k}}(e^{-\Delta D_{\mathbf{k}}/2} U_{\mathbf{k}}^\dagger \mathcal{F}_{\mathbf{r} \rightarrow \mathbf{k}}[\phi_j(\mathbf{r})]) \right] \quad (\text{B10})$$

with  $\mathcal{F}$  ( $\mathcal{F}^{-1}$ ) denoting the Fourier transform in the forward (backward) direction, with the following convention for a function  $f(\mathbf{r})$ :  $\mathcal{F}_{\mathbf{r} \rightarrow \mathbf{k}}[f] = \frac{1}{V} \int d\mathbf{r} \exp(-i\mathbf{k} \cdot \mathbf{r}) f(\mathbf{r})$ .

Collecting all factors, we arrive at a partition function  $\mathcal{Z} = \int \mathcal{D}(\tilde{\phi}, \tilde{\phi}^\dagger) e^{-S[\tilde{\phi}, \tilde{\phi}^\dagger]}$  with the discrete imaginary time action for the Rashba boson system  $S[\tilde{\phi}, \tilde{\phi}^\dagger] = S_0[\phi, \phi^\dagger] + S_{\text{int}}[(\phi, \phi^\dagger)']$ :

$$S_0[\tilde{\phi}, \tilde{\phi}^\dagger] = \sum_{\mathbf{k}} \sum_{j=0}^{N_\tau-1} \tilde{\phi}_{j,\mathbf{k}}^\dagger [\tilde{\phi}_{j,\mathbf{k}} - e^{-\Delta D_{\mathbf{k}}} \tilde{\phi}_{j-1,\mathbf{k}}] \quad (\text{B11})$$

$$S_{\text{int}}[(\phi, \phi^\dagger)'] = \frac{\Delta}{2} \sum_{j=0}^{N_\tau-1} \int d\mathbf{r} \sum_{\alpha\gamma} g_{\alpha\gamma} \phi_{\alpha,j}^*(\mathbf{r})' \phi_{\gamma,j}^*(\mathbf{r})' \phi'_{\alpha,j-1}(\mathbf{r})' \phi'_{\gamma,j-1}(\mathbf{r}) \quad (\text{B12})$$

which is studied in the main text.

As discussed in the main text, it is advantageous to conduct CL in the diagonalized basis. Since the unitary transformation does not modify the functional integral measure, we can prescribe the same off-diagonal descent Langevin scheme for coherent states in the dressed basis:

$$\frac{\partial \tilde{\phi}_{j,\mathbf{k}}}{\partial t} = -\frac{\delta S[\tilde{\phi}, \tilde{\phi}^*]}{\delta \tilde{\phi}_{j,\mathbf{k}}^*} + \eta_{j,\mathbf{k}} \quad (\text{B13})$$

$$\frac{\partial \tilde{\phi}_{j,\mathbf{k}}^*}{\partial t} = -\frac{\delta S[\tilde{\phi}, \tilde{\phi}^*]}{\delta \tilde{\phi}_{j,\mathbf{k}}} + \eta_{j,\mathbf{k}}^* \quad (\text{B14})$$

where  $\eta_{j,\mathbf{k}}$  and  $\eta_{j,\mathbf{k}}^*$  are diagonal, complex-conjugate noise vectors which are constructed in real space with two independent real noise source fields:  $\eta_{\alpha,j}(\mathbf{r}, t) = \eta_{\alpha,j}^{(R)}(\mathbf{r}, t) + i\eta_{\alpha,j}^{(I)}(\mathbf{r}, t)$  and  $\eta_{\alpha,j}^*(\mathbf{r}, t) = \eta_{\alpha,j}^{(R)}(\mathbf{r}, t) - i\eta_{\alpha,j}^{(I)}(\mathbf{r}, t)$ , where the real and imaginary parts are generated independently with the following statistics  $\langle \eta_{\alpha,j}^A(\mathbf{r}, t) \eta_{\gamma,j'}^B(\mathbf{r}', t') \rangle = \delta_{j,j'} \delta_{A,B} \delta_{\alpha,\gamma} \delta(\mathbf{r} - \mathbf{r}') \delta(t - t')$ .

Importantly, the interaction part of the action is a function of propagated fields in the pseudospin basis, so we provide clarification on how to obtain the correct expressions for the thermodynamic forces required for Langevin sampling. For the  $\phi$  CL equation, the functional derivatives for the  $S_{\text{int}}$  portion of the action are determined by carefully including the appropriate Jacobian factors and transformations:

$$\begin{aligned} \frac{\delta S_{\text{int}}[(\phi, \phi^*)']}{\delta \tilde{\phi}_{j,\mathbf{k}}^*} &= e^{-\Delta D_{\mathbf{k}}/2} \left( \frac{\delta S_{\text{int}}[(\phi, \phi^*)']}{\delta (\tilde{\phi}_{j,\mathbf{k}}^*)'} \right) \\ &= e^{-\Delta D_{\mathbf{k}}/2} \left( \frac{\delta (\phi_{\mathbf{k}}^*)'}{\delta (\tilde{\phi}_{\mathbf{k}}^*)'} \right) \left( \frac{\delta S_{\text{int}}[(\phi, \phi^*)']}{\delta (\phi_{j,\mathbf{k}}^*)'} \right) \\ &= e^{-\Delta D_{\mathbf{k}}/2} U_{\mathbf{k}} \left( \frac{\delta S_{\text{int}}[(\phi, \phi^*)']}{\delta (\phi_{j,\mathbf{k}}^*)'} \right) \\ &= e^{-\Delta D_{\mathbf{k}}/2} U_{\mathbf{k}} \mathcal{F}_{\mathbf{r} \rightarrow \mathbf{k}} \left[ \frac{\delta S_{\text{int}}[(\phi, \phi^*)']}{\delta \phi_j^*(\mathbf{r})'} \right] \end{aligned}$$

where we have used the Jacobian  $U_{\mathbf{k}}$  for the dressed state transformation. For the force on  $\phi^*$ , we find the following:

$$\begin{aligned} \frac{\delta S_{\text{int}}[(\phi, \phi^*)']}{\delta \tilde{\phi}_{j,\mathbf{k}}} &= e^{-\Delta D_{\mathbf{k}}/2} \left( \frac{\delta S_{\text{int}}[(\phi, \phi^*)']}{\delta (\tilde{\phi}_{j,\mathbf{k}})'} \right) \\ &= e^{-\Delta D_{\mathbf{k}}/2} \left( \frac{\delta S_{\text{int}}[(\phi, \phi^*)']}{\delta (\phi_{j,\mathbf{k}})'} \right) \left( \frac{\delta (\phi_{\mathbf{k}})'}{\delta (\tilde{\phi}_{\mathbf{k}})'} \right) \\ &= e^{-\Delta D_{\mathbf{k}}/2} \left( \frac{\delta S_{\text{int}}[(\phi, \phi^*)']}{\delta (\phi_{j,\mathbf{k}})'} \right) U_{\mathbf{k}}^\dagger \\ &= \mathcal{F}_{\mathbf{r} \rightarrow \mathbf{k}} \left[ \frac{\delta S_{\text{int}}[(\phi, \phi^*)']}{\delta \phi_j(\mathbf{r})'} \right] U_{\mathbf{k}}^\dagger e^{-\Delta D_{\mathbf{k}}/2}. \end{aligned}$$

From here, the usual expressions for the functional derivative of the interacting portion of the action from reference ([13, 28]) may be used.

### Appendix C: Estimation of Observables

Under the exact quadratic propagator treatment, computing observables during Langevin sampling requires a modified procedure. A central finding of this work is that observables should be computed using the propagated coherent state fields  $(\phi, \phi^*)'$  with the functionals derived previously in the primitive first-order approach [13]. In other words, the functionals from the primitive approach

are reused with the substitution  $(\phi, \phi^*) \rightarrow (\phi, \phi^*)'$ , enabling straightforward implementation in existing software. Below we discuss the supporting arguments for this conclusion.

For a local observable  $\hat{O}(\mathbf{r})$ , the procedure for developing an estimator functional of the coherent state fields  $\hat{O}[\phi, \phi^*; \mathbf{r}]$  involves augmenting the Hamiltonian with an infinitesimal source field  $J(\mathbf{r})$  conjugate to the observable, so that  $\hat{H} \rightarrow \hat{H} + \hat{H}_J$  with  $\hat{H}_J = -\beta^{-1} \int d\mathbf{r} J(\mathbf{r}) \hat{O}(\mathbf{r})$  [13]. When retracing the steps to derive the field theory, one could choose to incorporate this source Hamiltonian with the interaction portion, leading to the matrix elements  $\langle \phi'_j | e^{-\Delta \hat{H}_{\text{int}}} e^{-\Delta \hat{H}_J} | \phi'_{j-1} \rangle$  to compute. Evaluating via a first-order Taylor expansion, we find that the operator functional would be evaluated using coherent state fields in the propagated basis, e.g.  $\tilde{O}[(\phi, \phi^*)] = O[(\phi, \phi^*)']$ . For example, a one-body observable  $\hat{O}$  is written using second quantized operators  $\hat{O} = \int d\mathbf{r} \psi^\dagger(\mathbf{r}) O(\mathbf{r}) \hat{\psi}(\mathbf{r})$  [35] and can be directly evaluated via this first-order accurate procedure. For instance, the density operator  $\hat{\rho}(\mathbf{r}) = \psi^\dagger(\mathbf{r}) \psi(\mathbf{r})$  leads to the density operator expression:

$$\frac{1}{Z} \frac{\delta Z[J]}{\delta J(\mathbf{r})} \Big|_{J=0} = \langle \tilde{\rho}[\phi, \phi^*; \mathbf{r}] \rangle \quad (\text{C1})$$

$$\tilde{\rho}[\phi, \phi^*; \mathbf{r}] = \frac{1}{N_\tau} \sum_{j=0}^{N_\tau-1} \phi_j^*(\mathbf{r})' \phi'_{j-1}(\mathbf{r}) \quad (\text{C2})$$

Spatial integration of this density functional recovers the expression for the total particle number from the main text, i.e.  $\tilde{N}[\phi, \phi^*] = \int d\mathbf{r} \tilde{\rho}[\phi, \phi^*; \mathbf{r}]$ , which is additionally verifiable by taking  $-\frac{\partial S}{\partial \mu}$ . This result implies that for a general operator that can be derived in this form – us-

ing an infinitesimal source field  $J(\mathbf{r})$  – the operator can be computed using the same expressions as before using the propagated coherent state fields instead. We emphasize that we additionally observe excellent accuracy at modest imaginary time discretizations for more complex observables, such as the superfluid density, pressure, and density structure factor.

#### Appendix D: Comparison to mean-field theory

Although both examples in our study are qualitatively in the mean-field regime with a high condensate fraction, both stochastic methods considered here are beyond mean-field in nature, capturing the impact of fluctuations on observables. Both the “primitive” propagator approach and our exact “quadratic propagator” method provide exact estimates of observables’ expectation values and include both quantum and thermal fluctuations [13]. A Gross-Pitaevski [24] or mean-field approach assumes one dominant configuration in the partition function, such that the BEC is governed by a semi-classical energy functional of the BEC macroscopic wavefunction. In Figure (4), we plot the estimate of each observable via mean-field theory, which assumes a fully condensed system at zero temperature. Thermodynamically, mean-field theory assumes the following relationship between the internal energy and the grand free energy:  $\langle U \rangle - \mu \langle N \rangle = \langle \Omega \rangle$ . Both Figure (4b) and (4d) show that this equality is violated, as expected at non-zero temperature. Beyond the scope of this study, however, would be a comparison of the mean-field results with a  $T = 0$  ground state method that includes quantum fluctuations.

---

[1] J. Shumway and D. M. Ceperley, *Le Journal de Physique IV* **10**, Pr5 (2000).

[2] T. Shen, Y. Liu, Y. Yu, and B. M. Rubenstein, *The Journal of Chemical Physics* **153**, 204108 (2020).

[3] B. M. Rubenstein, S. Zhang, and D. R. Reichman, *Physical Review A* **86**, 053606 (2012).

[4] T. Shen, H. Barghathi, J. Yu, A. Del Maestro, and B. M. Rubenstein, *Physical Review E* **107**, 055302 (2023).

[5] D. M. Ceperley, *Reviews of Modern Physics* **67**, 279 (1995).

[6] D. M. Ceperley and E. L. Pollock, *Physical Review Letters* **56**, 351 (1986).

[7] D. M. Ceperley and E. L. Pollock, *Physical Review B* **39**, 2084 (1989).

[8] C. M. Herdman, P.-N. Roy, R. G. Melko, and A. D. Maestro, *Nature Physics* **13**, 556 (2017).

[9] C. M. Herdman, A. Rommal, and A. Del Maestro, *Physical Review B* **89**, 224502 (2014).

[10] T. Hayata and A. Yamamoto, *Physical Review A* **92**, 043628 (2015).

[11] E. C. McGarrigle, K. T. Delaney, L. Balents, and G. H. Fredrickson, *Physical Review Letters* **131**, 173403 (2023).

[12] F. Attanasio and J. E. Drut, *Physical Review A* **101**, 033617 (2020).

[13] G. H. Fredrickson, K. T. Delaney, G. H. Fredrickson, and K. T. Delaney, *Field-Theoretic Simulations in Soft Matter and Quantum Fluids*, International Series of Monographs on Physics (Oxford University Press, Oxford, New York, 2023).

[14] R. P. Feynman, *Reviews of Modern Physics* **20**, 367 (1948).

[15] S. A. Chin and C. R. Chen, *The Journal of Chemical Physics* **117**, 1409 (2002).

[16] G. Semeghini, H. Levine, A. Keesling, S. Ebadi, T. T. Wang, D. Bluvstein, R. Verresen, H. Pichler, M. Kalinowski, R. Samajdar, A. Omran, S. Sachdev, A. Vishwanath, M. Greiner, V. Vuletić, and M. D. Lukin, *Science* **374**, 1242 (2021).

[17] N. R. Cooper, J. Dalibard, and I. B. Spielman, *Reviews of Modern Physics* **91**, 015005 (2019).

[18] X. Li, E. Zhao, and W. Vincent Liu, *Nature Communications* **4**, 1523 (2013).

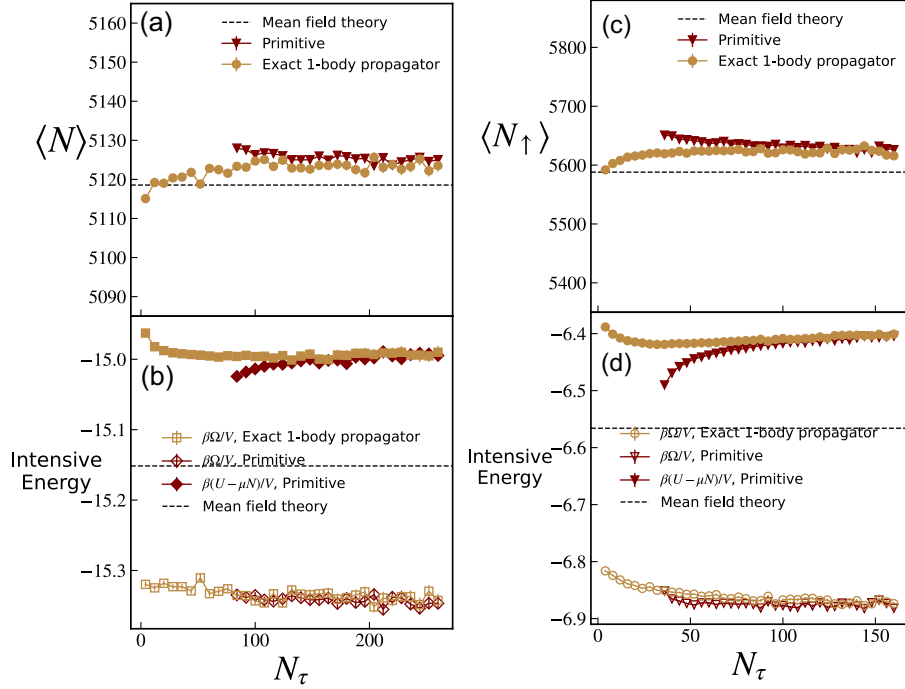


FIG. 4. Comparison of the results from the main text with mean-field theory references for both the a), b) single-component homogeneous Bose gas and the c), d) Rashba spin-orbit coupled Bose gas in the stripe phase. The mean-field reference for the corresponding observables are plotted in the black dashed line in all cases.

- [19] A. Valdés-Curiel, D. Trypogeorgos, Q.-Y. Liang, R. P. Anderson, and I. B. Spielman, *Nature Communications* **12**, 593 (2021).
- [20] J.-R. Li, J. Lee, W. Huang, S. Burchesky, B. Shteynas, F. C. Top, A. O. Jamison, and W. Ketterle, *Nature* **543**, 91 (2017).
- [21] T. Bland, E. Poli, C. Politi, L. Klaus, M. A. Norcia, F. Ferlaino, L. Santos, and R. N. Bisset, *Physical Review Letters* **128**, 195302 (2022).
- [22] M. A. Norcia, C. Politi, L. Klaus, E. Poli, M. Sohmen, M. J. Mark, R. N. Bisset, L. Santos, and F. Ferlaino, *Nature* **596**, 357 (2021).
- [23] B. Mukherjee, A. Shaffer, P. B. Patel, Z. Yan, C. C. Wilson, V. Crépel, R. J. Fletcher, and M. Zwierlein, *Nature* **601**, 58 (2022).
- [24] L. Pitaevskii and S. Stringari, *Bose-Einstein Condensation and Superfluidity* (Oxford University Press, 2016).
- [25] L. Pollet, *Reports on Progress in Physics* **75**, 094501 (2012).
- [26] K. W. Mahmud, E. N. Duchon, Y. Kato, N. Kawashima, R. T. Scalettar, and N. Trivedi, *Physical Review B* **84**, 054302 (2011).
- [27] B. Capogrosso-Sansone, S. G. Söyler, N. Prokof'ev, and B. Svistunov, *Physical Review A* **77**, 015602 (2008).
- [28] K. T. Delaney, H. Orland, and G. H. Fredrickson, *Physical Review Letters* **124**, 070601 (2020).
- [29] P. Heinen and T. Gasenzer, *Physical Review A* **106**, 063308 (2022).
- [30] N. Goldman, G. Juzeliūnas, P. Öhberg, and I. B. Spielman, *Reports on Progress in Physics* **77**, 126401 (2014).
- [31] A. Manchon, H. C. Koo, J. Nitta, S. M. Frolov, and R. A. Duine, *Nature Materials* **14**, 871 (2015).
- [32] V. Galitski and I. B. Spielman, *Nature* **494**, 49 (2013).
- [33] E. C. McGarrigle, R. Nodel, K. T. Delaney, L. Balents, and G. H. Fredrickson, *Physical Review A* **110**, L041303 (2024).
- [34] J. W. Negele and H. Orland, *Quantum Many-particle Systems* (Basic Books, 1988).
- [35] A. L. Fetter and J. D. Walecka, *Quantum Theory of Many-Particle Systems* (Courier Corporation, 2012).
- [36] S. Sachdev, *Quantum Phase Transitions* (Cambridge University Press, 2001).
- [37] X. Man, K. T. Delaney, M. C. Villet, H. Orland, and G. H. Fredrickson, *The Journal of Chemical Physics* **140**, 024905 (2014).
- [38] See supplementary material for additional details on the transformation of coherent-state wavefunctions under quadratic propagators, the application of this approach to rashba spin-orbit-coupled bosons, and the estimation of observables in coherent state complex langevin simulations.
- [39] C. Gerry and P. Knight, *Introductory Quantum Optics* (Cambridge University Press, Cambridge, 2004).
- [40] P. Blasiak, A. Horzela, K. A. Penson, A. I. Solomon, and G. H. E. Duchamp, *American Journal of Physics* **75**, 639 (2007).
- [41] S. Gopalakrishnan, I. Martin, and E. A. Demler, *Physical Review Letters* **111**, 185304 (2013).
- [42] R. M. Wilson, B. M. Anderson, and C. W. Clark, *Physical Review Letters* **111**, 185303 (2013).
- [43] R. E. Zillich, J. M. Mayrhofer, and S. A. Chin, *The Journal of Chemical Physics* **132**, 044103 (2010).
- [44] E. C. McGarrigle, H. D. Ceniceros, and G. H. Fredrickson, *Physical Review E* **110**, 065308 (2024).

- [45] A. Kamenev, *Field Theory of Non-Equilibrium Systems* (Cambridge University Press, 2011).
- [46] M. Doi, Journal of Physics A: Mathematical and General **9**, 1465 (1976).
- [47] L. Peliti, Journal de Physique **46**, 1469 (1985).
- [48] M. Fixman, The Journal of Chemical Physics **45**, 785 (1966).
- [49] Y.-J. Lin, K. Jiménez-García, and I. B. Spielman, Nature **471**, 83 (2011).
- [50] D. L. Campbell and I. B. Spielman, New Journal of Physics **18**, 033035 (2016).